Identification of pigments in different layers of illuminated manuscripts by X-ray Fluorescence mapping and Raman spectroscopy

S. Mosca, T. Frizzi, M. Pontone, R. Alberti, L. Bombelli, V. Capogrosso, A. Nevin, G. Valentini, D. Comelli

PII: S0026-265X(15)00268-4
DOI: doi: 10.1016/j.microc.2015.10.038
Reference: MICROC 2297

To appear in: *Microchemical Journal*

Received date: 31 July 2015
Revised date: 26 October 2015
Accepted date: 26 October 2015

Please cite this article as: S. Mosca, T. Frizzi, M. Pontone, R. Alberti, L. Bombelli, V. Capogrosso, A. Nevin, G. Valentini, D. Comelli, Identification of pigments in different layers of illuminated manuscripts by X-ray Fluorescence mapping and Raman spectroscopy, *Microchemical Journal* (2015), doi: 10.1016/j.microc.2015.10.038

Identification of pigments in different layers of illuminated manuscripts by X-ray Fluorescence mapping and Raman spectroscopy

S. Mosca[1*], T.Frizzi[2], M. Pontone[3], R. Alberti[2], L. Bombelli[2], V. Capogrosso[1], A. Nevin[4], G. Valentini[1], D. Comelli[1]

(1) Politecnico di Milano, Physics Department, Piazza Leonardo da Vinci 32, I-20133 Milano, Italy
(2) XGLab Srl, Via Francesco D'Ovidio 3, I-20131 Milano, Italy
(3) Archivio Storico Civico e Biblioteca Trivulziana, Castello Sforzesco, Piazza Castello 1, I-20121 Milano, Italy
(4) Istituto di Fotonica e Nanotecnologie - Consiglio Nazionale delle Ricerche (IFN-CNR), Piazza Leonardo da Vinci 32, I-20133 Milano, Italy

Corresponding Author

*Sara Mosca
Mailing: Politecnico di Milano, Physics Department, Piazza Leonardo da Vinci 32, I-20133 Milano, Italy
Email: sara.mosca@polimi.it ; Phone: +39 02 23996589

KEYWORDS:

1- Illuminated manuscripts
2- In-situ non-invasive analysis
3- X-ray fluorescence (XRF) mapping
4- Raman spectroscopy
5- Multivariate analysis

ABSTRACT
We propose a non-invasive approach for the study of illuminated manuscripts based on the combination of near-infrared reflectance imaging, X-Ray fluorescence mapping and Raman spectroscopy. Taking advantage of the different absorption coefficient of the characteristic X-ray emission lines of a specific element, we have implemented a differential mapping method to distinguish the X-ray emissions from two paint layers of a manuscript. This approach was applied to a coat-of-arms of a precious illuminated manuscript belonging to the Trivulziana library collection and revealed specific patterns through the mapping of the spatial distribution of lead in different paint layers. Multivariate methods, including principal component analysis and non-negative matrix factorization, applied to the X-Ray fluorescence mapping dataset demonstrate the spatial correlation between different elements. The use of complementary Raman and X-ray fluorescence spectroscopy has hence permitted the identification of the pigments employed in the original and overpainting layers found on the coat-of-arms. Through analysis, it was possible to identify the patron of the Salterium, attributed to Fracesco dei librai, as 15th C. bishop Bernardo de' Rossi.

1. Introduction

Illuminated manuscripts are precious written documents enriched by detailed decorations and miniature illustrations. The term '*illumination*' originally denoted the embellishment of the text with gold or, more rarely, silver. In the Middle Ages they were considered as status symbols for the owner, due to their intricate details, the cost of constituent materials and the complexity of the employed drawing techniques (1). This work focuses on the analysis of a late 15th C. Renaissance manuscript from the Trivulziana library collection based on the integration between Raman spectroscopy and X-ray fluorescence (XRF) spectroscopic mapping.

The attribution of a manuscript to a specific artist is often hampered by the fact that illuminated manuscripts are often unsigned or created in a workshop by multiple hands. Thus, for the purpose of attribution and dating, philological, historical and stylistic studies are often complemented with scientific analysis, with the latter mainly devoted to pigment identification. Manuscripts are delicate and fragile in comparison with other types of artworks: hence, beside the fact that micro-sampling is generally impossible, in-situ analysis is preferred with respect to non-invasive laboratory methods to avoid the transportation of precious books to environments without climate control.

The use of scientific analysis on illuminated manuscripts with a variety of spectroscopic techniques has been recently reviewed (2). A multi-analytical approach, based on in-situ elemental and molecular spectroscopic techniques, XRF, Raman and fiber-optic reflectance spectroscopy (FORS), can reveal pigment composition, even when materials are present as complex mixtures (3) (4) (5) (6) (7) (8). In order to overcome the limitations of the analysis of selected points, which may not be representative of a complex palette, methods for the study of an entire manuscript page have been further proposed. Delaney et al (9) employed near-infrared multispectral imaging combined with multivariate analysis to map areas of an illuminated manuscript painted with different colors. Pigment identification was than achieved following XRF and FORS of selected points. The use of XRF mapping (10), and its combination with Raman point analyses (11), has been proposed for detecting the spatial distribution of pigments in illuminated manuscripts.

While much work has focused on the analysis of pigments, less attention has been paid to the study of overpainting in illuminated manuscripts. In some cases coats of arms or symbols may be repainted following changes in property. Hence, during the investigations care must be paid to distinguish different painted layers in order to properly recover the history of the manuscript. Within this context, we propose a novel approach based on the complementary information provided by XRF spectroscopic mapping and remote Raman spectroscopy, aimed at identifying pigments and studying their spatial distribution in different layers of an illuminated manuscript. The approach is based on two different considerations. First, Raman and XRF spectroscopy are well recognized to yield complementary information for pigment identification, revealing the molecular structure and the elemental composition of pigments, respectively (12). Effective applications of this combined approach include the characterization of the colour palette of paintings (13), manuscripts (14) (15) (16), and printed works (17). Second, the high penetration depth of X-rays makes XRF sensitive to elements present in different sub-layers of a painted artwork. The use of XRF mapping devices for the visualization of underdrawings and *pentimenti* has already been reported, providing valuable and impressive results (18) (19), although studies have been limited to paintings on panels or canvas rather than on parchment or paper.

In the definition of our in-situ protocol care has been taken in order to avoid possible damages to delicate manuscripts. In recent years increasing attention has been dedicated to study the radiation effect induced by spectroscopic techniques which employ intense radiation sources, including lasers or synchrotrons (20). Although most of these techniques are considered to be non-destructive, the interaction of intense electromagnetic fields may induce chemical or physical changes in materials, which may be invisible by the naked eye. It is well-known that care must be taken during Raman spectroscopic analysis of heat sensitive pigments. This is particularly relevant when the material of interest is prepared in very thin and leanly bound paint layers, as is usual in illuminated manuscripts. For this purpose, the in-situ Raman device employed in this work is based on a remote probe, rather than on a conventional micro probe. Our system uses a lower fluence on the surface in comparison with conventional micro-probes, because its long-focal-length lens provides a spot on the sample which is a few hundred micrometers wide, large enough to prevent overheating. Analysis on standard samples has been carried out in order to validate the use of the remote probe and has been followed by the analysis of spots on the manuscript.

2. Materials and Methods

2.1 Painted model samples

Model samples made of a single painted layer, have been prepared by applying a pigment, dispersed in a binding medium made of casein, glycerine and linseed oil, on a canvas support with a lead white preparation layer. The painted layer has a thickness of about 500 – 700 µm. Pigments, binders and canvas support were purchased from Kremer Pigments (Aich stetten, Germany). The full list of analysed samples is provided in Table 1. Even though the material composition (pigments, binders and support) of the prepared model samples is not typical of historical illuminated manuscripts, spectroscopic analysis of them has provided useful information for evaluating the effectiveness of our approach.

2.2 The illuminated manuscript

The manuscript, known as the *Salterium* (Triv.2161) (21), is a precious illuminated manuscript, belonging to the Trivulziana library collection, with miniature illustration characteristic of the end of the 15th century, written in Greek and Latin by the same hand. The manuscript is on parchment and is 201 mm x 113 mm. Historical studies suggest that the manuscript come from the North of Italy (22). Much attention has been paid to the decorative apparatus, which have been attributed mostly to an artist known as Francesco dai librai (23), an Italian miniaturist who lived in Verona in the second half of the 15th C. The presence of some specific decorative elements, such as a bishop's mitre over each coat-of-arms with the initials B R in gold, suggest that the work was commissioned by a prominent figure (23). In this work we report analyses which aimed at identifying the manuscript patron. For the purpose, the coat-of-arms, located on the bottom part of different pages of the manuscript was analysed in detail (Figure.1a). All the measurements have been performed in-situ in the research laboratory of the Trivulziana Library.

2.3 Near-infrared reflectance imaging

Preliminary near-infrared (NIR) reflectance imaging has been performed for the rapid inspection of hidden details and overpainting. The set-up uses two halogen lamps (500 W), which uniformly illuminate the field of view, and a low-noise Si-based camera (Retiga 2000R, Qimaging) equipped with a fast camera lens (focal length = 50 mm, F# = 1.2, Nikon Europe). Infrared images of selected details of the manuscript have been recorded by mounting a transmission long-pass filter at 1 µm (FEL1000, Thorlabs Inc.) in front of the camera sensor. The absolute quantum efficiency of the camera beyond 1 µm, which is close to 1 %, is nonetheless sufficient to detect images of hidden details with a good contrast employing an acquisition time between 100 and 500 ms.

2.4 XRF mapping

The novel XRF mapping device employed in the present study is based on a portable commercial XRF spectrometer (Elio, XGLAB Srl) coupled to a XYZ translator stage. The XRF head employs a 25 mm^2 active area Silicon Drift Detector and a 50kV-4kW X-ray tube generator based on a Rh anode. The excitation X-ray beam is collimated to a 1.2 mm spot diameter on the sample surface at a working distance of ~ 1.4 cm. The typical energy resolution of the spectrometer is below 135 eV and elements from Na to Ur can be detected. Elemental 2D mapping of the sample surface is achieved through automatic XY raster scanning. The translator stage can cover a maximum area of 10 × 10 cm^2 with high accuracy (30 µm). With respect to other XRF mapping devices (19) (24), the compact head and the absence of any X-ray optics make it easily usable for in situ studies while providing good sensitivity even to lighter elements. XRF spectra of model samples and of selected points of the manuscript have been acquired with experimental conditions optimized to detect a good XRF emission from light elements: tube voltage variable from 20 to 50kV, tube anode current variable from 40 to 200µA, acquisition time = 60 s. Mapping measurements on the illuminated manuscript have been performed employing a tube voltage of 50kV, a tube anode current of 80µA and an acquisition time of 1 s for each point. The largest XRF map, 36 × 34 mm^2 with a lateral step of 800 µm, has been recorded in 45 mins. During XRF measurements the manuscript has been kept open, with the page of interest tilted to approximately 140 ° (Figure.1.b) to avoid the detection of the X-ray emission from underlying pages.

The spatial distribution of specific emission line of an element is reconstructed by mapping the related peak amplitude. In case of overlapping peaks, the peak of interest is fitted with a Gaussian curve within a proper region of interest.
The retrieved elemental maps have been further post-processed with multivariate analysis. Principal Component Analysis (PCA) has been applied to the correlation matrix of a dataset of the most significant elemental maps. Following this it is possible to better investigate the spatial correlation between elements belonging to the same pigment, or pigment mixture, which aids interpretation of the palette. In order to extract further information, which cannot be retrieved through analysis of elemental maps, a non-negative matrix factorization (NMF) has been applied to the whole raw XRF dataset. NMF is a dimension-reduction technique, which allows the approximation of a spectral dataset **X** (made of *n* XRF spectra described by *m* energy variables) into the linear composition of *k* non-negative spectral components weighted by proper non-negative weights. The decomposition is obtained through the minimization of the norm of the difference (**X** – **W**·**H**), where the *k* columns of the *n*-by-*k* matrix **W** represent transformations of the original variables in **X** and the *k* rows of the *k*-by-*m* matrix **H** represent the coefficients of the linear combinations of the original *m* variables in **X** that produce the transformed variables in **W** (25). The advantage of using NMF on XRF data with respect to more conventional multivariate methods (including PCA (26) (27) relies on the fact that NMF guarantees the extraction of nonnegative components, which respect the non-negativity of physical quantities and allows the attribution of a physical meaning to the factor decomposition.

2.5 Raman Spectroscopy

Raman measurements have been performed with a device described elsewhere (28). The device works in backscattering mode and employs a 785 nm CW laser source and a spectrometer (Acton SpectraPro2150, Princeton Instruments), mounting two alternative gratings (600 or 1200 grooves/mm), coupled to a cooled CCD camera (iDUS DV401A, Andor Technology Ltd.). A remote-probe, connected to the excitation laser and to the spectrometer through fibre optics, allows the analysis of a point of interest of 0.5 mm in diameter at a working distance of 30 cm (28). Alternatively, a micro-probe, based on a 20× objective that allows analysis of a circular spot of 50 μm in diameter at a working distance of ~ 3 mm, can be employed. Both the probes have been used for analysis of the painted model samples, whereas only the remote-probe has been used for in-situ measurements, avoiding contact with the analysed surface. Moreover, thanks to the larger spot size respect to the one achieved with the conventional Raman micro-probe, the surface receives a lower irradiance, reducing the risk of possible thermal damage.
In this work, Raman spectra have been collected in the spectral region from 150 to 3000 cm^{-1} with a spectral resolution of 20 cm^{-1} and 10 cm^{-1} with the remote- and the micro-probe, respectively. Measurements with the remote-probe have been carried out with a variable acquisition time between 15 to 40 s and irradiance on sample between 15 and 55 W/cm^2. Raman measurements with the micro-probe have been carried out with an acquisition time between 5 to 20 s and a irradiance on sample between 200 and 1500 W/cm^2.
Raman spectra are shown following spectral calibration and baseline correction. The identification of pigments was made through comparison with Raman data from published databases (29) (30) (31) and literature (32) (33) (34) (35).

3. Results and discussion

3.1 Analysis of painted model samples

Results of Raman and XRF analysis of model samples are reported in Table 1. By employing the remote-probe with maximum irradiance of 55 W/cm^2 all the painted samples, except the standard cobalt green, have at least one clearly detectable Raman marker. In terms of energy fluence induced on samples, it is of interest to remark that with the remote-probe it is possible to record meaningful Raman spectra employing fluence values lower by a variable factor between 7 to 100 respect to the micro probe. An example of the different performance of the Raman remote and micro-probe is seen in the analysis of the orpiment pigment (Figure 2). The remote-probe detects the Raman spectrum with a more intense baseline, which

gives rise to a lower signal-to-noise ratio. It is further evident that close Raman spectral lines (185, 202 cm^{-1}) can be detected only with the micro-probe thanks to its better spectral resolution. Nevertheless, these shortcomings do not hamper the identification of the pigment with the remote-probe, since the most intense vibrations are still visible.

Results from analysis of model samples corroborate the need for complementary XRF data when employing the Raman remote-probe. The effectiveness of the combined approach is reported for the analysis of Cobalt blue: whereas the Raman spectrum shows the presence of only a partially visible Raman signals related to the pigment (Table 1), the detection of Co and Al greatly increases the level of confidence for pigment identification. Conversely, Raman spectroscopy is crucial for the identification of other blue pigments, Cu-Phthalocyanine blue ($Cu,C_{32}H_{18}N_8$) and azurite ($2CuCO_3.Cu(OH)_2$). The two materials are characterized by similar XRF spectra but can be discriminated and identified on the basis of their Raman spectra.

As mentioned above, the high penetration depth of X-rays makes the XRF spectroscopy technique sensitive to elements distributed in different paint layers. This feature, which can be considered a strength of the X-ray-based spectroscopic method, becomes a serious drawback when analysing data recorded on unknown stratified samples. Indeed, in the XRF spectra of model samples lead is often observed, which is actually related to the preparation layer (white lead) and not to the superficial pigment. Here the integration of information provided by Raman spectroscopy (which is sensitive to surface layers) is of great importance for correctly separating the components of each painted layer.

3.2 Analysis of the illuminated manuscript

NIR reflectance imaging from the bottom part of page cv.3 (Figure.1a) suggests the presence of a figure of a lion under the blue coat-of-arms, which is not visible to the naked eye (Figure 3). The hidden figure can be related to the emblem of the original patron, intentionally masked and overpainted following a change in ownership of the book. Close examination of the NIR reflectance image demonstrates that the blue overpainting is not homogeneous and appears thinner or even absent in an area close to the left borders of the coat-of-arms.

Results of XRF mapping in reconstructed elemental maps of specific elements of the coat-of-arms are shown in Figure 4. The results of Raman analysis on selected points from the coat of arms are reported in Table 2.

The elemental maps of Al, Si, S, Ca and K are all correlated with the dark blue upper layer, whereas the spatial map of the Pb-Mα emission line closely resembles the spatial features of the red chevron (in heraldry reproduced as a wide inverted V) on the overpainted coat-of-arms. Bands in Raman spectra acquired from blue point on the centre of the coat-of-arms and on a red point of the chevron are attributed to Ultramarine Blue ($(Na,Ca)_8(AlSiO_4)_6(SO_4,S,Cl)_2)_4$) and Red Lead ($Pb_3O_4$) (Figure 5). Regarding the former, the presence of elements extraneous to the pigment composition, including Ca and K, suggest the use of a natural ultramarine blue pigment in the overpainted coat-of-arms, with Ca related to a contamination from other minerals (36) and K to the use of potassium carbonate in the traditional pigment manufacturing process.

The combined use of XRF mapping and Raman analysis indicates the use of Cinnabar pigment (HgS) for the red border of the emblem, identified through the Hg-Mα X-line emission and Raman bands at 253, 282 and 343 cm^{-1} (Figure 5). The spatial distribution of Hg in the coat-of-arm (figure 4.d), reveals two spots, not visible with the naked eye in the colour image of the miniature (Figure 4.a, arrowed), probably related to the claws of the paws of the hidden lion figure.

The background of the lion figure is spatially correlated with the distribution of Cu, indicating that the original background was painted with a copper-based pigment. The identification of the pigment is provided by Raman spectroscopy: the spectrum detected on a point of the coat-of-arms close to the left border, where the blue overpainting layer seems absent, indicates the use of Azurite (Figure 5).

PCA performed on a dataset of the most relevant elemental maps provides additional information. Here, the first two PCs account for the 99.6 % of the variance of the dataset; Figure 6, where original variables (XRF detected elements) are shown as vectors, gives a graphical representation of how each variable

contributes to the two PCs: it can be observed a strong spatial correlation of Al, Si, Na, K and Ca confirms the presence of natural Ultramarine Blue $(Na,Ca)_8(AlSiO_4)_6(SO_4,S,Cl)_2$); instead, the other which elements are spatially uncorrelated and hence related to different pigments. It is of interest to observe that the emission from the two different lines of Pb (-Lα and -Mα) are not strongly correlated, and the reason for this will be addressed below.

The hidden figure of the lion detected by NIR reflectance imaging is visible in the elemental map of the Pb-Lα emission line, indicating the use of a Pb-based pigment for this hidden decoration. Indeed, in this map the spatial features of the chevron are visible. The chevron is painted with Red Lead, which partially masks the underlying lion figure. In order to separate the two layers, both painted with lead-based pigments, we have exploited the difference in the X-ray absorption coefficients of different emission lines of lead, as already proposed by others (37) (38) (39). In our case, we have considered the different absorption coefficients of the Pb-Lα and -Mα lines. The energetic emission from Pb-Lα line (10.3 keV), being poorly attenuated, is related to lead elements present in the whole stratigraphy of the miniature; on the other hand the detected emission from Pb-Mα line (2.38 keV) is related to surface layers only since photons emitted in underlying layers are strongly absorbed by upper layers.

In order to quantify this effect in the analysis of the coat of arms, we have assumed a simple bi-layer model made of an upper ultramarine layer, of thickness *h*, over a semi-infinite lead layer. The probability of detecting a photon generated within the lead layer is given by $e^{-\mu\rho h}$, where μ is the mass attenuation coefficient (at a certain energy line) of a top layer of density ρ. The upper layer has been modelled as a homogeneous dispersion of ultramarine blue in water at 20 % wt, which yields a density $\rho=1.3$ g/cm^3 and an attenuation coefficient μρ at the Pb-Lα and -Mα lines of 29 cm^{-1} and 1.13×10^3 cm^{-1}, respectively (40). With this model, after 50 μm the emission from Pb-Mα line is completely attenuated (Figure 7), whereas photons from Pb-Lα line are attenuated only by 15%.

The differential map of the Pb-Lα and Pb-Mα emission lines has been calculated by taking into account the different detector efficiency at the two energy lines of lead: ΔPb= Pb-Lα - *k*.Pb-Mα. The normalization factor *k* has been estimated from a point of the scanned area presumably made of a single painting layer and is close to 4. The retrieved ΔPb map (Figure.8) clearly reveals the figure of the hidden lion, painted with a lead-based pigment, whose colour cannot be resolved on the basis of the present elemental analysis.

A clear visualization of the two layers in terms of elemental composition is provided by combining proper elemental maps in two false colour RGB maps (Figure9.a and 9.b): in addition to preliminary NIR reflectance imaging, which has allowed the simple identification of the hidden figure of a lion, the combined elemental and molecular spectroscopy approach has permitted the identification of the pigment composition of the coat-of-arms at two different layers: Cinnabar, Azurite and a lead-based pigment in the original coat-of-arms, natural Ultramarine Blue and Red Lead in the overpainting. With the proposed colour distribution of the hidden decoration and in the light of previous historical studies (Section 2.2), the coat-of-arms can be identified as that of the de' Rossi family (Figure.9c), a white lion on a red-bordered blue background, allowing the attribution of the original owner of the manuscript to Bernardo de'Rossi (who was Bishop of Belluno from 1488 and Treviso from 1499). On the basis of this final finding, we hypothesise that the lion figure had been painted with a lead-based white pigment, probably Lead White. Interestingly, the pigments used for the upper layer, which were commonly used in European manuscripts and miniatures, suggests that the overpainting is not a modern one.

Considering the high-level of dimensionality and the redundancy of information of the raw dataset retrieved through XRF mapping, we finally tested the effectiveness of NMF decomposition for mapping pigments. The method has been applied to the largest XRF mapping dataset recorded in the present research, which comprises the coat-of-arms, the surrounding angels and the mitre (made of 45 × 43 pixels and 4095 energy variables). The dataset is decomposed in the linear combination of 5 energy dispersed spectra multiplied by the maps that show the spatial distribution of the corresponding weights (Figure10). The first two energy dispersed spectra include mainly the emission lines of Pb and Cu, respectively. The other energy dispersed spectra are a combination of different elements (i.e. Pb + Ca, Au + Pb and Hg +

Ca in spectra 3, 4 and 5 respectively) and the related maps give insight on their co-localization. Specifically, spectrum 4 maps the features of the angels' hair, of a detail of the mitre and of the inscription in the upper part of the XRF map, suggesting the presence of Pb together with Au in details where gilding has been applied.

4. Conclusion

In this work we have shown how XRF mapping helps in identifying the distribution of pigments in both surface and hidden layers of an illuminated manuscript. Indeed, the difference in the X-ray absorption coefficients of different emission lines of a specific element, already considered by other authors (37) (38), can be used to differentiate X-ray emissions from different layers of a painted artwork. Nevertheless, the attribution of a specific element to a certain layer of a painting is not straightforward when performed with a point-like device and often requires the use of proper theoretical model of X-rays propagation and Monte Carlo simulations (41). Conversely, here we show how the approach is particularly effective when applied with a mapping or imaging device, since the provided spatial information is essential for detecting the morphology of different painted layers. Statistical methods based on non-negative matrix factorization for the analysis of data from XRF mapping are powerful for the separation of contributions from different pigments in complex images. The integration of data from XRF and Raman spectroscopies is of great value not only for the identification of a pigment, but also for the correct attribution of a pigment to a superficial or to a hidden layer. Finally, the proposed remote-Raman device allows the use of a lower irradiance on sample surface respect to conventional micro-probe, without limiting the capability of the technique for pigment identification, a particularly critical feature for the analysis of fragile artworks in light of recent studies of mitigation strategies for radiation damage in the analysis of ancient and precious works (20).

The spatial resolution of the XRF mapping approach is limited with respect to the level of detail required for the full understanding of the hidden paint layers – and for this reason other imaging approaches including NIR are required. Alternative approaches for XRF imaging based on the use of full field detectors combined with a pin hole would allow higher resolution spectral images (42). Further, the remote-Raman probe (28) also includes a 2D scanning device, which has not been used in the present study due to time constraints. Nevertheless, this feature could be exploited to achieve a vibrational map of the area of interest that would highly complement XRF mapping data. The combination of elemental and vibrational mapping would further increase the effectiveness of the proposed approach for the in-situ study of illuminated manuscripts and paintings.

5. Acknowledgements

The authors are grateful to Cristina Morganti and Arkedos srl for the preparation of the standard sample. Research was partially funded by the Italian Ministry of Education, Universities and Research within the framework of the JPI Cultural Heritage − JHEP Pilot call through the LeadART project "Induced decay and aging mechanisms in paintings: focus on interactions between lead and zinc white and organic material", and by Regione Lombardia within the framework of the Regional Operative Program 2007-2013 through the "Smart Culture" project.

Bibliography

1. J. J.Bradley, Illuminated Manuscripts, London, Bracken Books, November 19, 2006.

2. S. Pessanha, M. Manso, M.L. Carvalho, Application of spectroscopic techniques to the study of illuminated manuscripts: A survey, Spectrochim. Acta - Part B At. Spectrosc. 71-72 (2012) 54–61. doi:10.1016/j.sab.2012.05.014.

3. K. Trentelman, N. Turner, Investigation of the painting materials and techniques of the late-15th century manuscript illuminator Jean Bourdichon, J. Raman Spectrosc. 40 (2009) 577–584. doi:10.1002/jrs.2186.

4. D.Bersani, P.P.Lottici, F. Vignali, G. Zanichelli, A study of medieval illuminated manuscripts by means of portable Raman equipments, J. Raman Spectrosc. 2006 and 37: 1012–1018, DOI: 10.1002/jrs.1593.
5. M. Aceto, A. Agostino, G. Fenoglio, A. Idone, M. Gulmini, M. Picollo, et al., Characterisation of colourants on illuminated manuscripts by portable fibre optic UV-visible-NIR reflectance spectrophotometry, Anal. Methods. 6 (2014) 1488. doi:10.1039/c3ay419.
6. P.Ricciardi, J.K Delaney, M.Facini, L.Glinsman, Journal of the American Institute for Conservation 52(1): 13-29. DOI: 10.1179/0197136012Z.0000000004.
7. S.Bruni, S.Caglio, V.Guglielmi, G. Poldi, The joined use of n.i. spectroscopic analyses-FTIR, Raman, visible reflectance spectrometry and EDXRF to study drawings and illuminated manuscripts, Appl. Phys. A Mater.Sci.Process. 92 (2008) 103–108. doi:10.1007/s00339-008-4454-x.
8. M. Aceto, A. Agostino, G. Fenoglio, M. Gulmini, V. Bianco, E. Pellizzi, Non invasive analysis of miniature paintings: Proposal for an analytical protocol, Spectrochim. Acta - Part A Mol. Biomol. Spectrosc. 91 (2012) 352–359. doi:10.1016/j.saa.2012.02.021.
9. J.K. Delaney, P. Ricciardi, L.D. Glinsman, M. Facini, M. Thoury, M. Palmer, et al., Use of imaging spectroscopy, fiber optic reflectance spectroscopy, and X-ray fluorescence to map and identify pigments in illuminated manuscripts, Stud. Conserv. 59 (2014). 91–101. doi:10.1179/2047058412Y.0000000078.
10. A. L.M. Silva, M.L. Carvalho, K. Janssens, J.F.C. a. Veloso, A large area full-field EDXRF imaging system based on a THCOBRA gaseous detector, J. Anal. At. Spectrom. 30 (2015) 343–352. doi:10.1039/C4JA00301B.
11. A. Deneckere, M. De Reu, M.P.J. Martens, K. De Coene, B. Vekemans, L. Vincze, et al., The use of a multi-method approach to identify the pigments in the 12th century manuscript Liber Floridus, Spectrochim. Acta - Part A Mol. Biomol. Spectrosc. 80 (2011). 125–132. doi:10.1016/j.saa.2011.03.005.
12. L. Burgio, D. a. Ciomartan, R.J.H. Clark, Pigment identification on medieval manuscripts, paintings and other artefacts by Raman microscopy: Applications to the study of three German manuscripts, J. Mol. Struct. 405 (1997) 1–11. doi:10.1016/S0022-2860(96)09422-7.
13. F. Rosi, C. Miliani, C. Clementi, K. Kahrim, F. Presciutti, M. Vagnini, et al., An integrated spectroscopic approach for the non-invasive study of modern art materials and techniques, Appl. Phys. A. 100 (2010) 613–624. doi:10.1007/s00339-010-5744-7.
14. A. Le Gac, S. Pessanha, S. Longelin, M. Guerra, J.C. Frade, F. Lourenço, et al., New development on materials and techniques used in the heraldic designs of illuminated Manueline foral charters by multi-analytical methods, Appl. Radiat. Isot. 82 (2013). 242–257. doi:10.1016/j.apradiso.2013.07.027.
15. T.D. Chaplin, R.J.H. Clark, M. Martinón-Torres, A combined Raman microscopy XRF and SEM-EDX study of three valuable objects,London, J. Mol. Struct. 976 (2010) 350–359. doi:10.1016/j.molstruc.2010.03.042.
16. A. Duran, M.L. Franquelo, M. a. Centeno, T. Espejo, J.L. Perez-Rodriguez, Forgery detection on an Arabic illuminated manuscript by micro-Raman and X-ray fluorescence spectroscopy, J. Raman Spectrosc. 42 (2011) 48–55.doi:10.1002/jrs.2644.
17. P. Zannini, P. Baraldi, M. Aceto, A. Agostino, G. Fenoglio, D. Bersani, et al., Identification of colorants on XVIII century scientific hand-coloured print volumes, J. Raman Spectrosc. 43 (2012) 1722–1728. doi:10.1002/jrs.4119.
18. J. Dik, K. Janssens, G. van der Snickt, L. van der Loeff, K. Rickers, M. Cotte, Visualization of a lost painting by Vincent van Gogh using synchrotron radiation based X-ray fluorescence elemental mapping, Analytical Chemistry 80 (2008) 6436–6442.
19. M. Alfeld, V. Pedroso, V.E. Hommes, G. Van, A mobile instrument for in situ scanning macro-XRF, J. Anal. At. Spectrom. 28 (2013) 760–767. doi:10.1039/c3ja30341a.
20. L. Bertrand, S. Schöeder, D. Anglos, M.B.H. Breese, K. Janssens, M. Moini, et al., Trends in Analytical Chemistry Mitigation strategies for radiation damage in the analysis of ancient materials, Trends Anal. Chem. 66 (2015) 128–145. doi:10.1016/j.trac.2014.10.005.

21. http://manus.iccu.sbn.it//opac_SchedaScheda.php?ID=210060., Censimento dei manoscritti delle biblioteche italiane. Manus online. [Online].
22. C.Santoro, I codici medioevali della Biblioteca Trivulziana, Milano 1965, pp. 272-315.
23. I.Fiorentini, Un salterio greco latino per il vescovo Bernardo de' Rossi, in Aldèbaran III. Storia dell'arte, a cura di S. Marinelli, Verona 2015, pp. 45-56.
24. M. Alfeld, K. Janssens, J. Dik, W. de Nolf, G. van der Snickt, Optimization of mobile scanning macro-XRF systems for the in situ investigation of historical paintings, J. Anal. At. Spectrom. 26 (2011) 899. doi:10.1039/c0ja00257g.
25. M.W. Berry, M. Browne, A.N. Langville, V.P. Pauca, R.J. Plemmons, Algorithms and applications for approximate nonnegative matrix factorization, Comput. Stat. Data Anal. 52 (2007) 155–173. doi:10.1016/j.csda.2006.11.006.
26. G. Sciutto, P. Oliveri, S. Prati, M. Quaranta, S. Bersani, R. Mazzeo, An advanced multivariate approach for processing X-ray fluorescence spectral and hyperspectral data from non-invasive in situ analyses on painted surfaces, Anal. Chim. Acta. 752 (2012). 30–38. doi:10.1016/j.aca.2012.09.035.
27. A. Deneckere, L. De Vries, B. Vekemans, L. Van De Voorde, F. Ariese, L. Vincze, et al., Identification of inorganic pigments used in porcelain cards based on fusing Raman and X-ray fluorescence (XRF) data, Appl. Spectrosc. 65 (2011) 1281–1290. doi:10.1366/11-06368.
28. A. Brambilla, I. Osticioli, A. Nevin, D. Comelli, C.D. Andrea, A. Brambilla, et al., A remote scanning Raman spectrometer for in situ measurements of works of art A remote scanning Raman spectrometer for in situ measurements of works of art, Rev. Sci. Instrum. 82 (2011). doi:10.1063/1.3600565.
29. http://rruff.info/, RRUFF Project website . [Online].
30. http://www.chem.ucl.ac.uk/resources/raman/, Raman Spectroscopic Library. UCL online. [Online].
31. http://www.ehu.eus/udps/database/database1.html, e-visart database. e-vibrational spectroscopic database. [Online].
32. I.M. Bell, R.J. Clark, P.J. Gibbs, Raman spectroscopic library of natural and synthetic pigments (pre-approximately 1850 AD)., Spectrochim. Acta. A. Mol. Biomol. Spectrosc. 53A (1997) 2159–2179. doi:10.1016/S1386-1425(97)00140-6.
33. P. Vandenabeele, B. Wehling, L. Moens, H. Edwards, M. De Reu, G. Van Hooydonk, Analysis with micro-Raman spectroscopy of natural organic binding media and varnishes used in art, Anal. Chim. Acta. 407 (2000) 261–274. doi:10.1016/S0003-2670(99)00827-2.
34. L. Burgio, R.J.H. Clark, Library of FT-Raman spectra of pigments, minerals, pigment media and varnishes, and supplement to existing library of Raman spectra of pigments with visible excitation, Spectrochim. Acta. A. Mol. Biomol. Spectrosc. 57A (2001). 1491–1531(21). doi:10.1016/S1386-1425(00)00495-9.
35. A.M. Correia, R.J.H. Clark, M.I.M. Ribeiro, L.T.S. Duarte, Pigment study by Raman microscopy of 23 paintings by the Portuguese artist Henrique Pousao (1859–1884), J. Raman Spectrosc. 38 (2007) 1280–1287. doi:10.1002/jrs.
36. I. Osticioli, N. Mendes, A. Nevin, F. Gil, M. Becucci, E. Castellucci, Analysis of natural and artificial ultramarine blue pigments using laser induced breakdown and pulsed Raman spectroscopy, statistical analysis and light microscopy,.Spectrochim. Acta - Part A Mol. Biomol. Spectrosc., 73 (2009) 525–531. doi:10.1016/j.saa.2008.11.028.
37. T. Trojek, T. Čechák, L. Musílek, Recognition of pigment layers in illuminated manuscripts by means of Kα/Kβ and Lα/Lβ ratios of characteristic X-rays, Appl. Radiat. Isot. 68 (2010) 871–874. doi:10.1016/j.apradiso.2009.09.054.
38. T. Cechak, L. Musilek, T. Trojek et al., Application of X-ray fluorescence analysis in investigations of historical monuments, 45 (2006) 48–51.
39. C. Fiorini, a. Gianoncelli, a. Longoni, F. Zaraga, Determination of the thickness of coatings by means of a new XRF spectrometer, X-Ray Spectrom. 31 (2002) 92–99. doi:10.1002/xrs.550.
40. -Ray form factor, Attenuatoin and scattering table. [Online] http://physics.nist.gov/PhysRefData/FFast/html/form.html.

41. T. Trojek, T. Čechák, L. Musílek, Techniques for depth heterogeneity identification in X-ray fluorescence, Nucl. Instruments Methods Phys. Res. Sect. B Beam Interact. with Mater. Atoms. 263 (2007) 76–78. doi:10.1016/j.nimb.2007.04.064.
42. F.P. Romano, C. Caliri, L. Cosentino, S. Gammino, L. Giuntini, D. Mascali, et al., Macro and Micro Full Field X-Ray Fluorescence with an X-Ray Pinhole Camera Presenting High Energy and High Spatial Resolution, Anal. Chem. 86 (2014) 10892–10899. doi:10.1021/ac503263h.

(a)

(b)

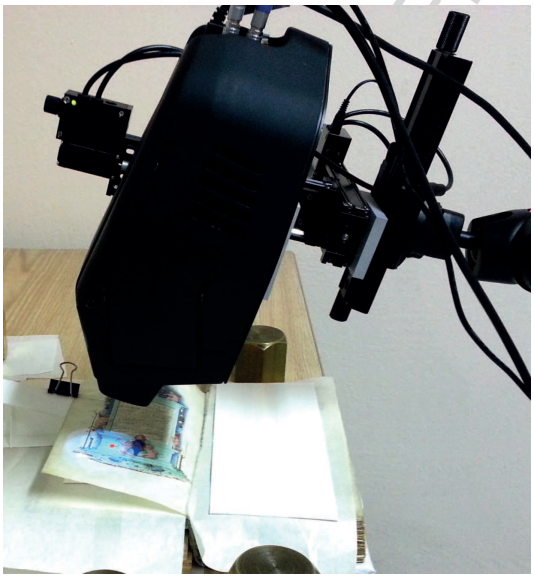

Figure 1

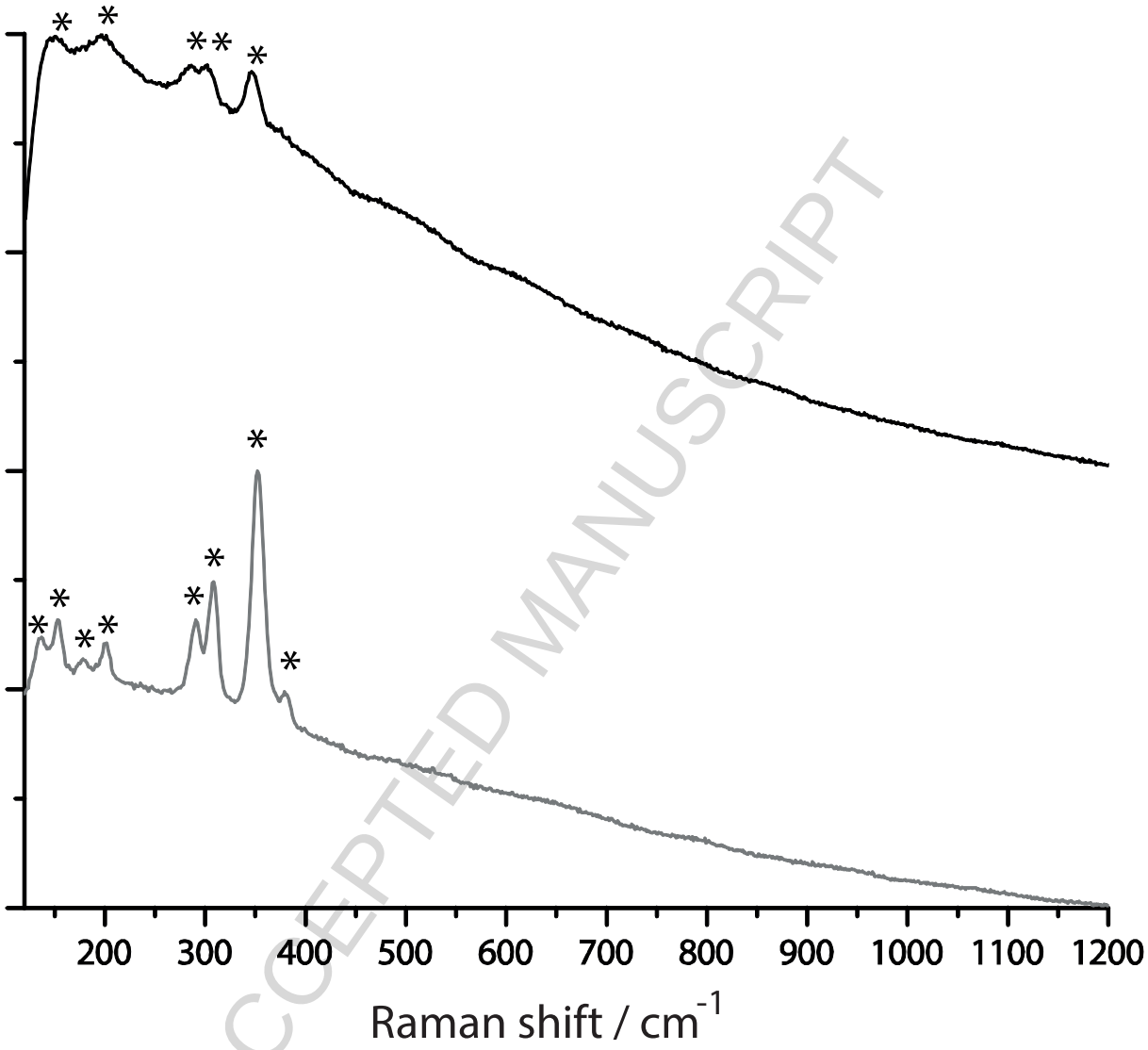

Figure 2

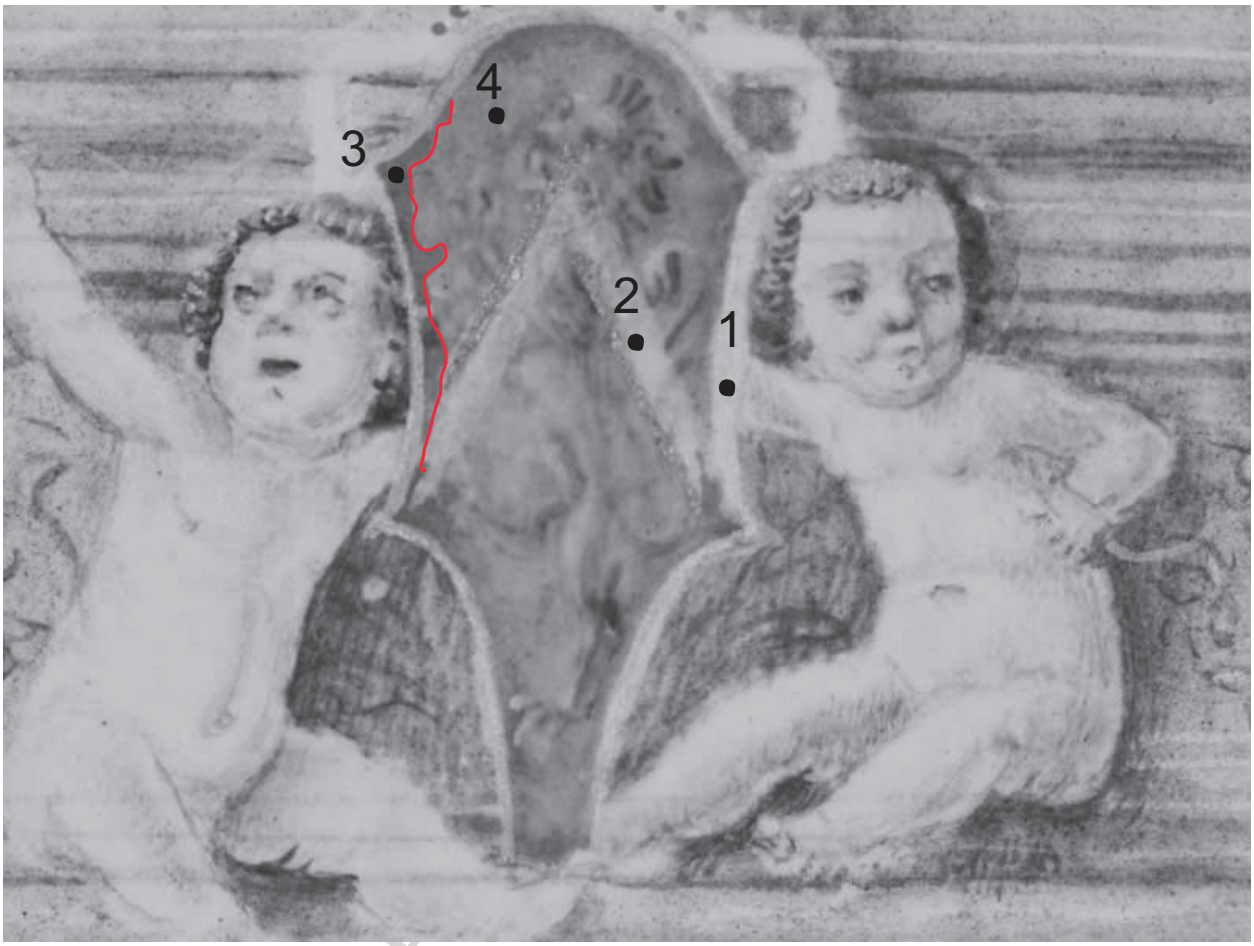

Figure 3

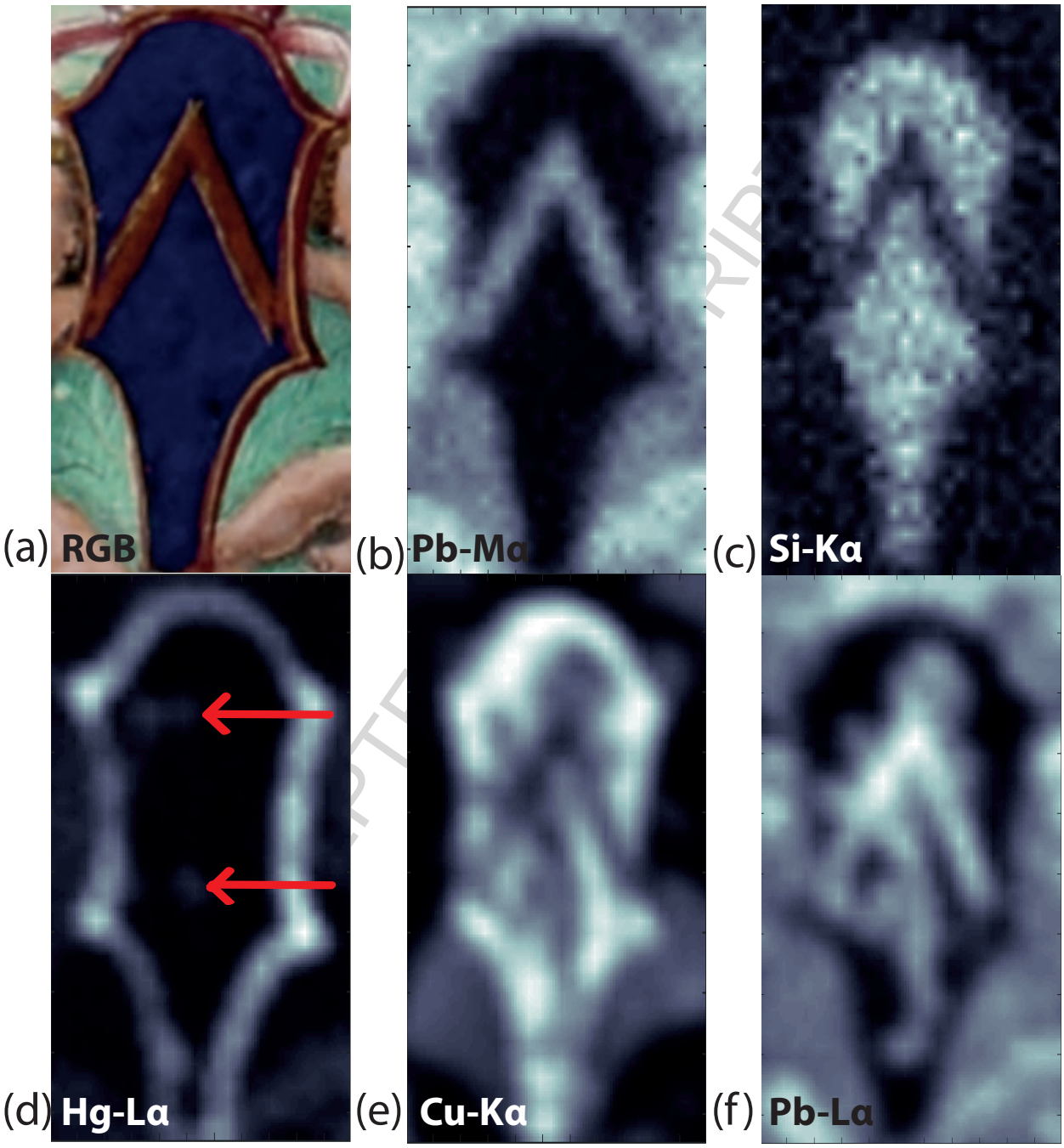

Figure 4

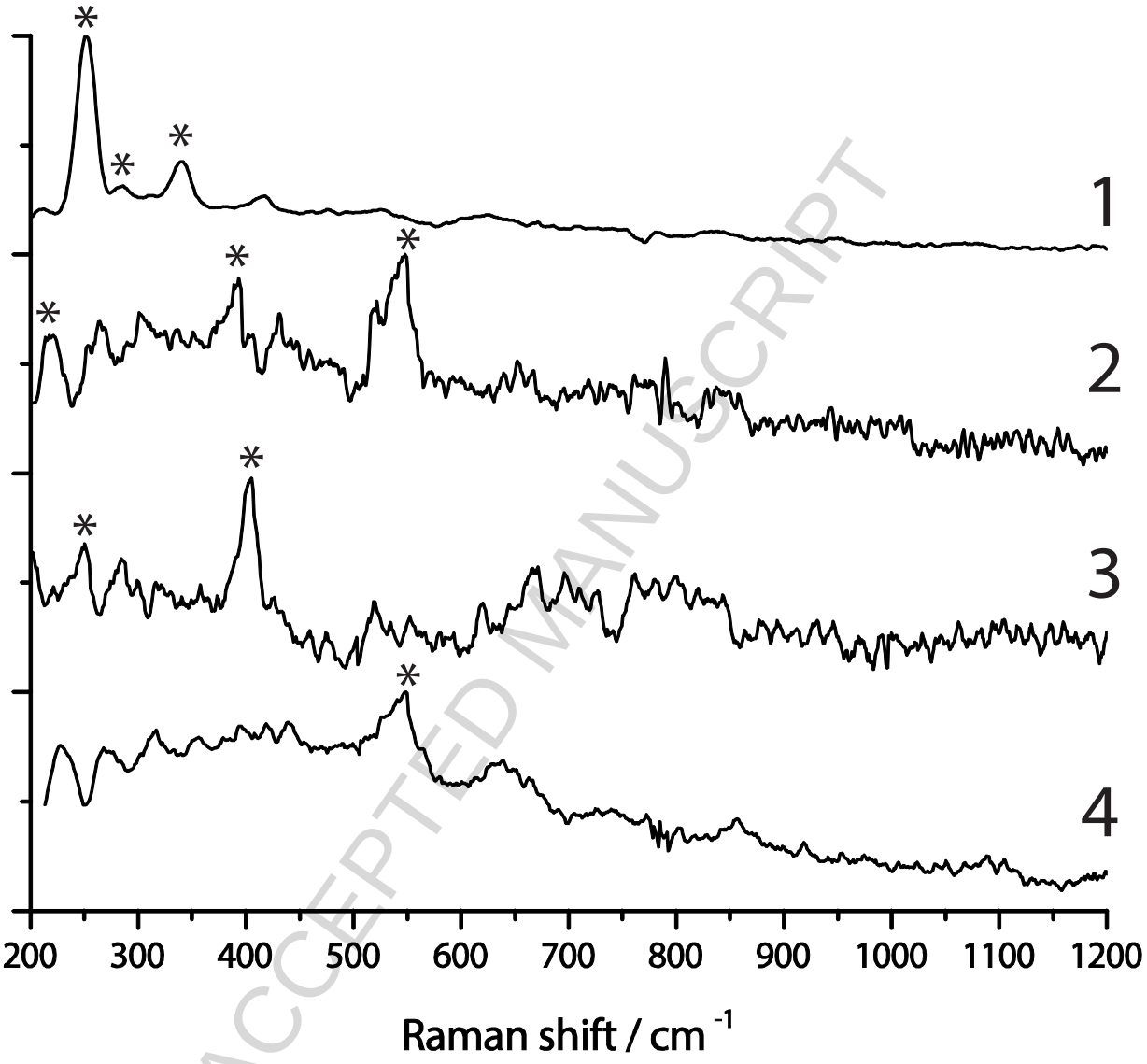

Figure 5

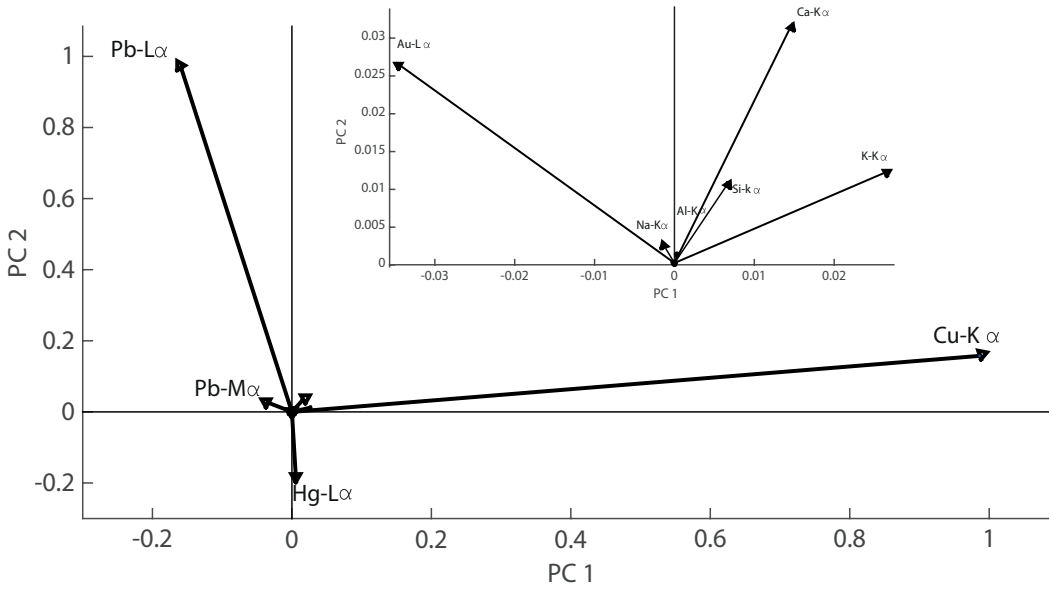

Figure 6

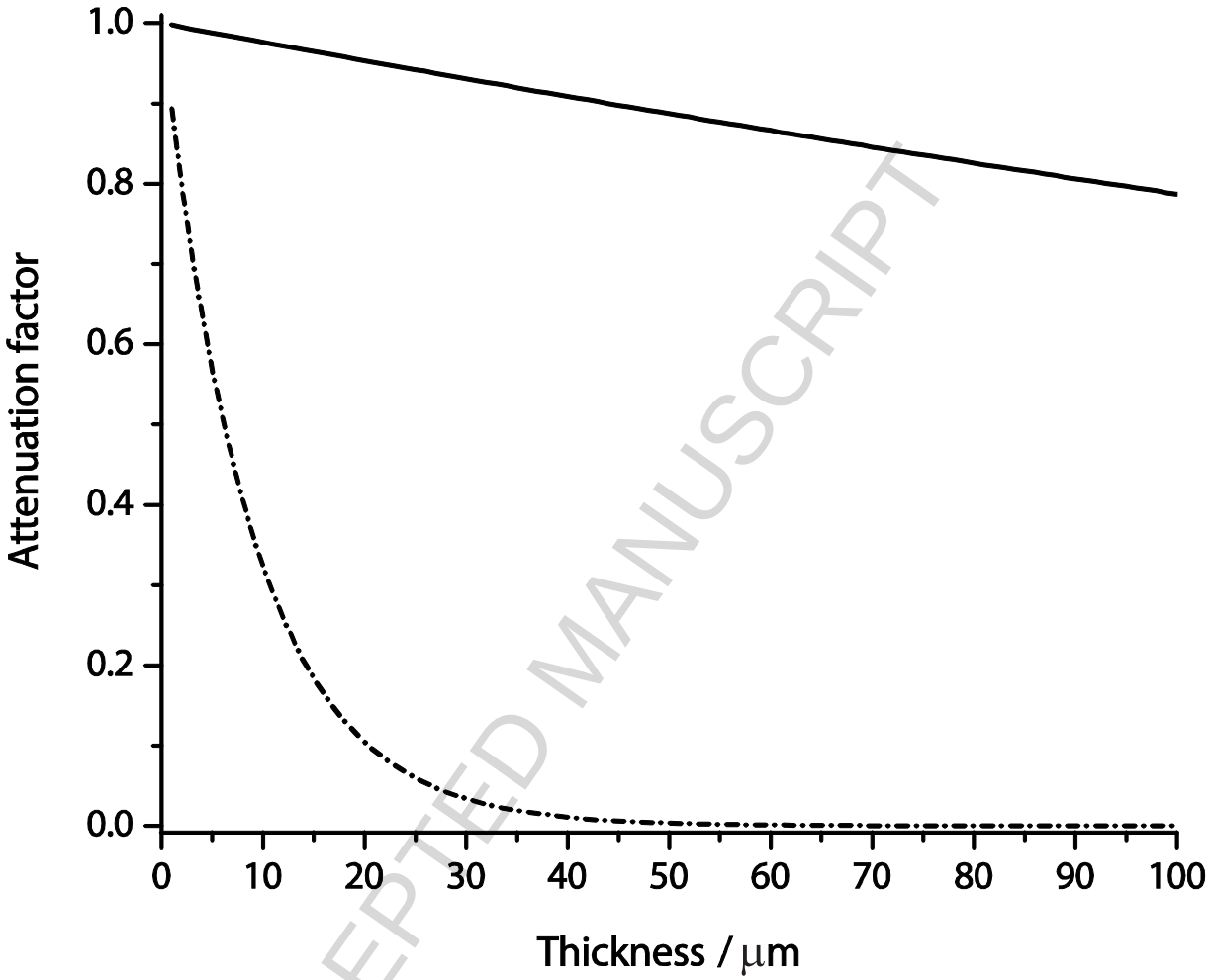

Figure 7

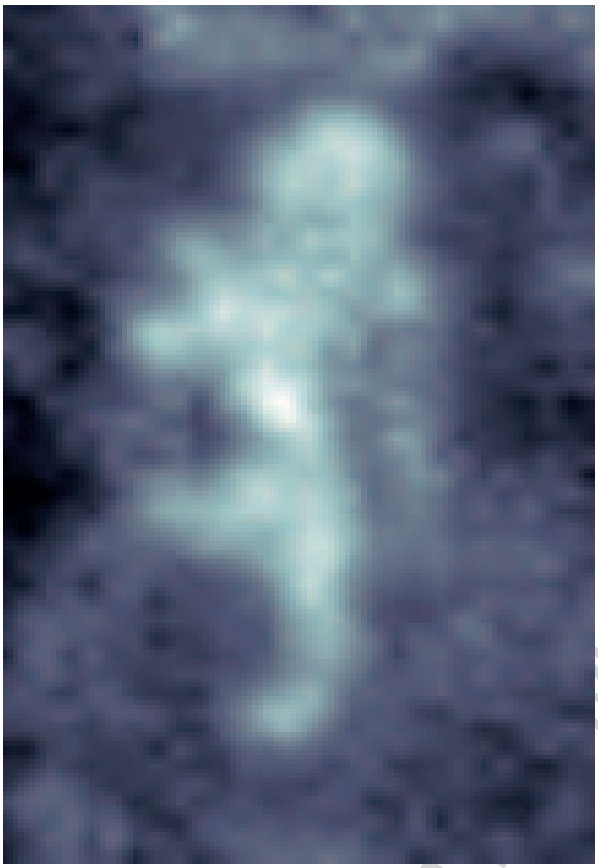

Figure 8

(a)

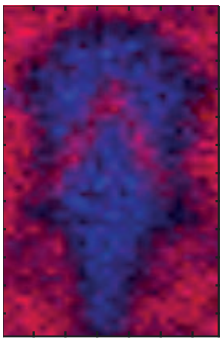

(b)

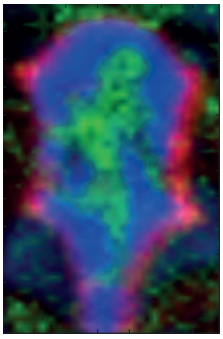

(c)

Figure 9

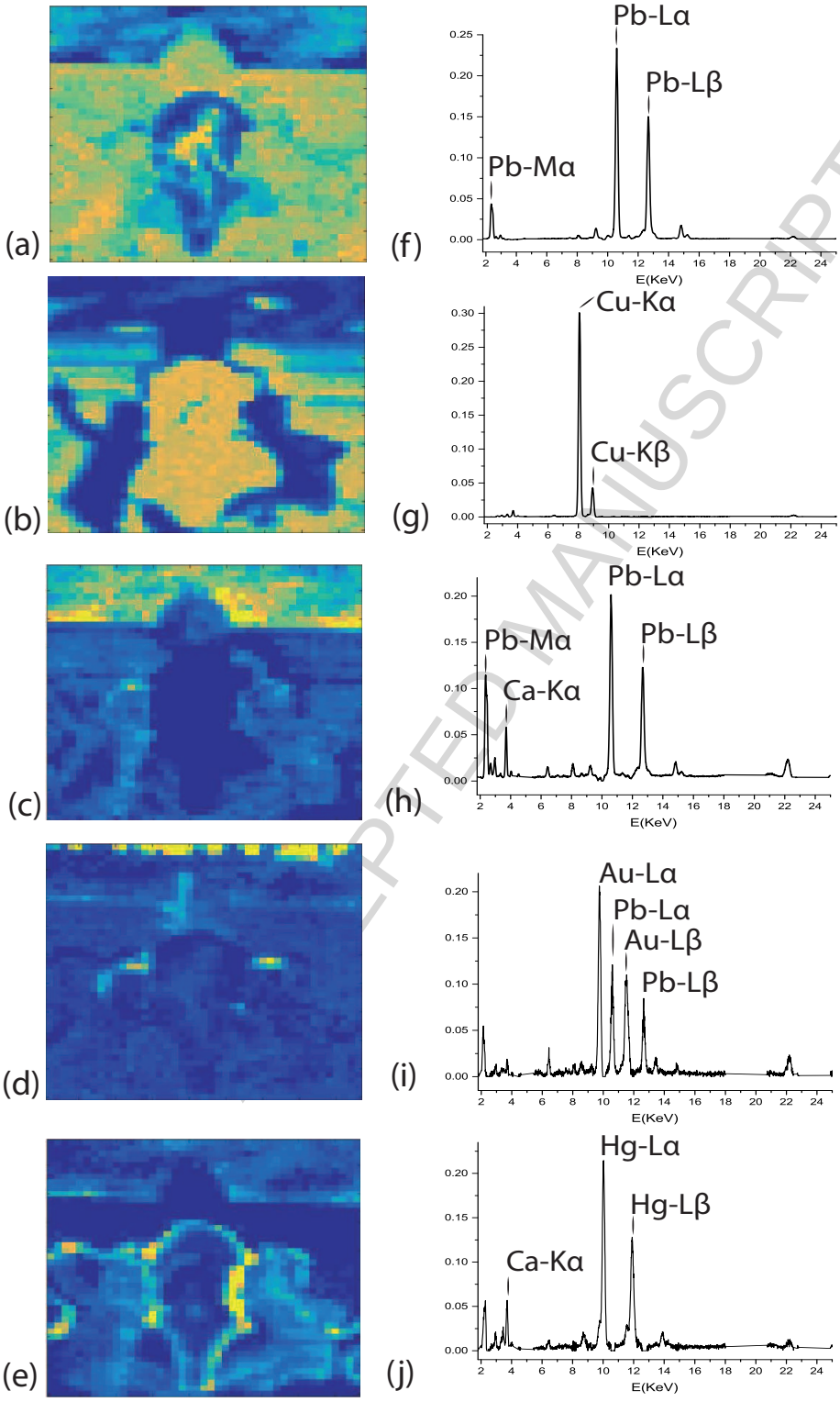

Figure 10

Tab.1 – List of the analyzed painted model samples and results of analysis provided by XRF spectroscopy (in terms of elements detected) and Raman spectroscopy (in terms of Raman vibrations detected) employing both the remote- and the micro-probe with the related experimental conditions. Elements detected by XRF spectroscopy shown in brackets are attributed to the lead white preparation layer. Raman bands are indicated as very strong (vs), strong (s), medium (m) and weak (w).

Name / Chemical formula	**Remote-probe**		**Micro-probe**		**XRF**
	Raman bands (cm^{-1})	**Energy density [J/cm^2] (Power density [W/cm^2]*acquisition time [s])**	**Raman bands (cm^{-1})**	**Energy density [J/cm^2] (Power density [W/cm^2]*acquisition time [s])**	**Detected elements**
Cerulean blue / $CoO.nSnO_2$	532 w, 674vw	160 (16*10)	495m; 532s; 674vs	1100 (220*5)	Co, Sn, Zn, Cr, (Pb)
Cobalt blue / $CoO.Al_2O_3$ $CoO.nSnO_2$	512 w,	210 (21*10)	203s, 512vs	4711 (673*7)	Co, Sn, Si, Al(tr), (Pb)
Ultramarine blue / $Na_8[Al_6Si_6O_{24}]S_n$	548s	250 (25*10)	548s,1096w	2750 (550*5)	Na, Si, S, (Pb)
Phtalocyanine blue / $C_{32}H_{18}N_8$	482s, 599m, 679s,746s, 1142w,1337vs, 1440w,1523v	160 (16*10)	256m, 482s, 599m, 679vs,746vs, 951m, 1142w, 1190w, 1337vs, 1440m, 1523vs	2700 (1350*2)	Cu, (Pb)
Azurite / $2CuCO_3.Cu(OH)_2$	401m	500 (25*20)	250m; 403vs; 1098m;	5500 (550*10)	Cu, (Pb)
Cobalt chromite green / $CoCr_2O_4$	No signal	480 (16*30)	987w, 717s, 527m, 488(b)m,	9750 (975*10)	Co, Cr, Ti, Ni, Zn, (Pb)
Red Lead / Pb_3O_4	122s; 149m; 223w; 313w; 390w; 548s	150 (30*5)	122vs; 149m; 223w; 313w; 390w; 548vs	2800 (1400*2)	Pb
Cinabar / HgS	252vs; 282w(sh); 343m	45 (9*5)	252vs; 282w(sh); 343m	1100 (1100*1)	Hg, S, (Pb)
Orpiment / As_2S_3	154s; 202w; 309m; 353s	18 (18*1)	136w; 154s; 181vw; 202w; 292m; 309s; 353vs; 381w	1700 (1700*1)	As, S, (Pb)
Lead tin yelllow type I / Pb_2SnO_4	129vs; 196m; 275w(br); 379w; 457m	140 (28*5)	129vs; 196s; 275w(b); 291w; 379w; 457m; 525w	8500 (1700*5)	Pb, Sn
Naples yellow / $Pb_2Sb_2O_7$	140s	550 (55*10)	140vs, 292s, 346m, 467s, 1052vw	11900 (1700*7)	Pb, Sb,

Tab.2 – List of the Raman bands identified in selected points of the illuminated manuscript (see figure 3) employing a power density of 20 W/cm^2 and an acquisition time of 30 s per point.

Point of analysis	**Color**	**Raman shift (cm^{-1})**	**Identified Pigment / Chemical formula**
1	Red	**252vs;** 282w (sh); 343m	Cinnabar / HgS
2	Red	223w, 390w; 480vw; **548vs**	Red lead / Pb_3O_4
3	Blue	250m; **403vs**; 1098m;	Azurite / $2CuCO_3.Cu(OH)_2$
4	Blue	**548vs;** 1096m	Ultramarine / $Na_{8-10}Al_6Si_6O_{24}S_{2-4}$

Figure 1. (a) Color image of page 7 (c. 3v) of the *Salterium* manuscript, cod. Triv. 2161, c.3v (Milano, Archivio Storico Civico e Biblioteca© Comune di Milano). All rights reserved with the coat-of-arms examined in the present study; the red and black squares point out the two areas analysed by XRF mapping. (b) Colour picture of the XRF-head during mapping measurements on the manuscript.

Figure 2. Raman spectra of the Oripiment-based model sample recorded with the remote (black line) and the micro-probe (gray line). For better clarity, each spectrum has been normalized to its maximum value and shifted in intensity. Asterisks highlight the Raman bands used for pigment identification.

Figure 3. NIR reflectance image of the coat-of-arms. The image reveals an underpainted layer depicting the figure of a lion. Black filled circles outline the points analyzed using Raman spectroscopy for the study of the blue and red pigments. The red closed line indicates an area of the background sublayer not completely covered by the overpainting blue layer.

Figure 4. (a) Color image of the detail of the coat-of-arms scanned with the XRF mapping device(see figure 1a, black square); (b)-(f) elemental maps reconstructed on the basis of XRF data recorded in the smaller area (14 × 24 mm^2, sampled with a lateral step of 500 µm). The red arrow underlines the presence of two spots in the Hg- map, probably related to the claws on the paws of the hidden lion figure.

Figure 5. Raman spectra recorded on four points on the coat-of-arm shown in figure 3. For better clarity, each spectrum has been normalized to its maximum value and shifted in intensity. Asterisks highlight the detected Raman bands related to the presence of Cinnabar (spectrum 1), Red Lead (spectrum 2), Azurite (spectrum 3) and Ultramarine Blue (spectrum 4).

Figure 6. Results of PCA performed on a dataset made of 10 XRF maps (Al-Kα, Au-Lα, Ca-Kα, Cu-Kα, Hg-Lα, K-Kα, Na-Kα, Pb-Lα, Pb-Mα) reconstructed on the coat-of-arms (see figure 1a, black square): graphical representation of the original variables (detected elements, displayed as vectors) plotted as coefficients of the first two PCs. In the inset, a zoomed view of the plot is given.

Figure 7. Reconstructed probability of detecting a photon, emitted in a lead sub-layer, versus the thickness of an ultramarine blue upper layer for the Pb-Lα (10.3 keV – solid black curve) and Pb-Mα emission energies (2.38 keV – dash dot black curve). Simulations have been performed assuming a semi-infinite lead sub-layer, which does not give rise to any absorption effect, and an upper layer, of variable thickness, painted with a 20% dispersion of ultramarine blue pigment (density = 1.3 g/cm^3) in water.

Figure 8. Differential map (ΔPb) obtained by properly subtracting the Pb-Mα elemental map from the Pb-Lα one.

Figure 9. (a) Reconstructed RGB image of the superficial upper layer of the coat-of-arms, created by combining the Pb-Mα (red channel) and Si-Kα (blue channel) elemental maps with the green channel set to 0; (b) reconstructed RGB image of the hidden layer of the coat-of-arms

created by combining the Hg-Lα (red channel), ΔPb (green channel) and Cu-Kα (blue channel) elemental maps; (c) detail of the cover of the portrait of Bernardo de' Rossi - "*Allegory of Virtue and Vice*" (Oil on panel, 1505, Washington, National Gallery of Art), containing the family coat-of-arms with a white lion on a blue background.

Figure 10. Results of NMF analysis on the XRF mapping dataset of the coat-of-arms (see Figure 1(a), red square) (36 x 34 mm^2 in size, lateral step = 800 μm) following spectral decomposition in 5 non-negative components; (a)-(e) score maps; (f)-(j) related energy dispersed spectra.

Highlights

- We propose a non-invasive approach to study illuminated manuscripts.
- We have implemented a differential mapping method to distinguish the X-ray emissions from different layers.
- We avoid possible damage thanks to a novel Raman device based on a remote probe.
- The combined use of Raman and X-ray fluorescence has permitted the identification of the pigments.
- We could identify the patron of the manuscript, who was a prominent bishop belonging to a 15th century clergy family.